THE ASTROPHYSICAL JOURNAL, 312:303–313, 1987 January 1

GROUND-BASED OBSERVATIONS OF *IRAS* CANDIDATES FOR LATE ASYMPTOTIC GIANT BRANCH STARS[1]

SUN KWOK[2]
Department of Physics, The University of Calgary
BRUCE J. HRIVNAK[2]
Department of Physics, Valpariso University and Dominion Astrophysical Observatory
AND
R. T. BOREIKO[2]
Department of Physics, The University of Calgary
Received 1986 January 21; accepted 1986 June 17

ABSTRACT

Ground-based infrared photometric observations were obtained for 16 of the *IRAS* Circular No. 9 sources which have been suggested to be candidates of OH/IR stars. Five of these sources are confirmed to be OH/IR stars and three others as carbon stars. Two are young objects in an early stage of star formation and one, possibly two, are planetary nebulae. Two sources of very low color temperatures ($\sim$180 K) are also found, and we suggest that they probably represent objects in transition between the asymptotic giant branch and planetary nebula phases.

Subject headings: infrared: sources — nebulae: planetary — stars: late-type

I. INTRODUCTION

The late stage of asymptotic giant branch (AGB) evolution remains one of the least understood phases of single star evolution. It is currently believed that as an intermediate mass (2–8 $M_\odot$) star ascends the AGB, it loses mass at an increasing rate and eventually completely obscures itself in a dust envelope that forms out of stellar wind material. The IRC and AFGL surveys have discovered a number of infrared objects which are evolved stars with such high optical depths in the circumstellar envelopes that the photospheres are totally unobservable. Comparison between the infrared spectra of these objects and evolved stars with optical counterparts (in particular Mira variables) suggests that there is an evolutionary sequence of increasing redness with age. This effect is clearly illustrated in oxygen-rich AGB stars, where the circumstellar 9.7 μm silicate feature can be seen to evolve from emission to self-absorption as the optical depth of envelope increases (Merrill 1977). The increase of optical depth with age is now generally interpreted as the result of increasing mass loss as the star reaches the final stages of the AGB.

Infrared observations of late AGB stars have been complemented by radio spectral-line observations, first in OH and H_2O masers and later in thermal CO emission. Generally, but not exclusively, late AGB stars which are oxygen-rich show OH emission whereas carbon-rich stars show CO emission (Knapp *et al.* 1982). Variability studies of OH/IR stars show that they have pulsation periods of 600 to 2000 days and can be considered as the extensions of optical Mira variables (Herman and Habing 1985; Engels *et al.* 1983). Late AGB stars have also been discovered by galactic OH surveys (Baud *et al.* 1985), and many of these objects are found to have only infrared but no optical counterparts.

It is possible, however, that there exist extremely late AGB stars which remained undetected in the previous infrared sky surveys because they emit predominantly at wavelengths beyond 20 μm. The *IRAS* sky survey therefore offers the opportunity to discover some of the most evolved stars at or near the end of AGB evolution. The *IRAS* properties of known OH/IR stars have been analyzed by Olnon *et al.* (1984), and *IRAS* Circular No. 9 (Habing and Olnon 1984) lists 33 objects which have flux ratios comparable to those of known OH/IR stars. In a previous paper (Hrivnak, Kwok, and Boreiko 1985, hereafter Paper I) we reported the identification of 16 of the 33 Circular No. 9 objects, and in this paper we report infrared photometric observations and discuss the possible nature of these objects.

II. OBSERVATIONS

Our observations were all made with the 3.6 m Canada-France-Hawaii Telescope (CFHT) on Mauna Kea. The f/35 infrared set-up for this telescope has been described by Maillard and Dyck (1982). Observing dates were 1984 August 12–16. The observations were made with a helium-cooled Ge bolometer with an aperture of 10".5 and a throw of 20" in declination. The characteristics of the broad-band filters used are listed in Table 1.

The objects were located by manually scanning the *IRAS* error boxes, as described in Paper I. Paper I also includes a finding chart for each object.

The primary star used to standardize our observations was α Lyr, which was observed two or three times each night. Since α Lyr is not a strong source at 20 μm and is very weak at 25 μm, additional infrared standards (α Her, β And, μ Cep) were also observed for calibration at these bands. The fluxes of the program objects were first corrected for extinction, and then transformed to standard magnitudes. For the wavelength interval 7.8–12.5 μm, α Lyr was used as the standard, and it was assumed to have a magnitude of 0.00 in each bandpass. At 20 μm the transformation was accomplished by using the three

[1] *Publication of the Rothney Astrophysical Observatory*, No. 38.
[2] Visiting Astronomer at the Canada-France-Hawaii Telescope, operated by the National Research Council of Canada, the Centre National de Recherche Scientifique of France, and the University of Hawaii.

TABLE 1

IR FILTER CHARACTERISTICS

Central Wavelength (μm)	FWHM (μm)	F_ν for 0.0 mag (Jy)
7.8	0.7	61
8.7	1.2	49
9.8	1.2	39
10.3	1.0	35
10.5	5.1	34
11.6	1.3	28
12.5	1.2	24
20	9	9.8
25	10	6.5

additional standards listed above, based upon the standard magnitudes found in Tokunaga (1984) and Hanner *et al.* (1984). At 25 μm standard magnitudes have not been published for any of these stars. Therefore, we estimated the absolute flux of the three additional standards by a linear extrapolation of their spectra on a plot of log F_λ vs. log λ, using the absolute flux calibation of Hanner *et al.* (1984). These 25 μm fluxes were then converted to the magnitude scale through a similar extrapolation of the absolute flux density for a 0.00 mag star. The conversion factors used to obtain flux densities from magnitudes are those by Hanner *et al.* and are listed in Table 1. There is evidence of some variability in two of the three standard stars used at the longer wavelengths, and we have therefore incorporated additional uncertainty into the error estimates of our final results.

The final standardized magnitudes of the program objects are listed in Table 2. Based on the signal-to-noise ratio of our observations and the uncertainties in standardization, we believe a conservative estimate of the accuracy of these magnitude values to be ± 0.10 at the shorter wavelengths, and ± 0.15 and ± 0.30 at 20 μm and 25 μm, respectively, except where noted otherwise. In two cases the objects were not detected at 25 μm, and upper limits were set at 3 σ.

III. RESULTS

Our 1984 CFHT observations were initiated based on information in *IRAS* Circular No. 9. Since then, the *IRAS Point Source Catalog* has been published and updated flux densities of the program sources were obtained from the catalog. Since the *IRAS* filters have broad bandpasses (Neugebauer *et al.* 1984), color corrections are necessary to obtain reliable flux values at the centers of the filters. The color temperatures (T_{ij}) are determined between adjacent *IRAS* bands i and j, and the correction factors are derived by interpolation using correction factors listed in Table VI.C.6 of the *IRAS Catalogs and Atlas Explanatory Supplement* (Beichman *et al.* 1985). For bands with two adjacent bands (25 and 60 μm), the two correction factors are averaged before they are applied. The corrected flux densities of the *IRAS* measurements and the color temperatures used for correction are given in Table 3.

Comparison of the *IRAS* 25 μm band fluxes with our measurements show that there are discrepancies for several objects. In most cases, they can be attributed to intrinsic variations of the sources. The majority of the sources in the *Point Source Catalog* were observed by *IRAS* at two epochs separated by 6 months, and thus variability can be detected. The last column of Table 3 lists the probability of variability for each of the program sources as listed in the *IRAS Point Source Catalog*, based on the 12 and 25 μm band fluxes measured at the two epochs. Most of the sources with discrepant fluxes are in fact variable sources. In some cases it may also be possible that we have resolved the source, for the *IRAS* aperture is much larger than ours.

19548+3035 and 02441+6922 are listed in the *IRAS Point Source Catalog* as associated with RAFGL 2477 and RAFGL 5081, respectively. A search of the *Catalog of Infrared Observations* (Gezari, Schmitz, and Mead 1984) shows that only 19548+3035 has previous ground-based observations. The CFHT observations show fluxes and colors comparable to those of the *IRAS* measurements, and we are confident that all 16 objects are correctly identified. The infrared spectra of the sources are plotted in Figures 1–3. In the five cases where the certainty of variability in a source is 80% or more, we have

TABLE 2

OBSERVATIONAL DATA

IRAS ID	Obs. Date (Dy-Mo-Yr)	Magnitudes								
		7.8 μm	8.7 μm	9.8 μm	10.3 μm	10.5 μm	11.6 μm	12.5 μm	20 μm	25 μm
19127+1717	16-08-84	2.26	1.98	1.75	1.67	1.69	1.05	0.95	−0.47	−0.6
19200+1536	16-08-84	3.34	3.42	3.82	...	3.10	2.40	2.04	0.65	−0.3[a]
19288+2923	14-08-84	0.95	0.86	1.19	1.10	0.68	0.27	−0.09	−1.25	−1.5
19374+2359	12-08-84	1.26	1.30	1.39	1.17	0.91	0.31	−0.10	−1.95	−2.7
19386+1513	14-08-84	1.45	0.58	−0.18	−0.20	0.12	−0.22	0.06	−1.34	−1.0
19454+2920	16-08-84	3.95	2.76	1.85	1.69	1.49	0.83	0.35	−1.98	−2.5
19477+2401	16-08-84	3.44	3.00	2.52	2.13	1.86	1.03	0.67	−0.97	−1.8
19520+2759	12-08-84	1.12	0.63	0.32	0.22	0.15	−0.41	−0.55	−2.35	−3.0
19548+3035[b]	12-08-84	−0.79	−1.30	−1.64	−1.73	−1.74	−2.22	−2.34	−3.35	−3.8
19558+3333	14-08-84	2.26	1.90	1.59	1.57	1.46	1.03	0.90	−0.27	−0.8
20103+3053	16-08-84	4.73	4.88	4.38	4.63	4.46	3.75	3.53	2.16	> −0.3
23268+6854	16-08-84	1.31	0.87	0.63	0.61	0.57	0.17	−0.03	−0.69	> −2.9
00170+6542	14-08-84	1.08	0.21	−0.30	−0.39	−0.10	−0.69	−0.55	−1.75	−1.9
00210+6221	14-08-84	1.61	1.00	0.67	0.58	0.56	0.04	−0.10	−0.94	−1.4
01133+6434	16-08-84	...	...	...	...	4.09	...	...	−0.82	−1.3[a]
02441+6922	14-08-84	2.38	1.92	1.46	1.36	1.44	1.03	1.37	−0.36	−0.8

[a] Error estimate of ± 0.5 mag.
[b] AFGL 2477.

TABLE 3

IRAS OBSERVATIONS

IRAS ID	T_{12}	T_{23} (K)	T_{34}	Corrected Flux Density (Jy) 12 μm	25 μm	60 μm	100 μm	Probability of Variability (%)
19127+1717.....	245	228	...	14.11	7.2	7.1	<7.3	0
19200+1536.....	232	211	...	7.12	10.0	4.5	<41.4	82
19288+2923.....	255	600	154	46.36	47.6	11.4	6.7	99
19374+2359.....	174	162	...	28.60	99.7	63.0	...	4
19386+1513.....	327	15144	...	40.50	25.9	3.4	<2.9	99
19454+2920.....	163	181	10182	20.76	90.3	44.0	13.3	23
19477+2401.....	166	211	...	13.57	53.8	22.9	<37.1	7
19520+2759.....	203	109	65	56.42	124.3	208.6	214.0	16
19548+3035.....	252	238	14966	86.37	98.8	37.0	12.7	99
19558+3333.....	292	453	...	47.22	38.5	9.8	<37.0	94
20103+3053.....	222	122	...	3.51	6.0	7.2	<21.3	99
23268+6854.....	259	128	351	30.51	36.0	36.7	16.4	4
00170+6542.....	276	997	...	30.49	26.4	5.3	<21.1	17
00210+6221.....	292	591	...	53.28	42.6	9.8	<22.7	15
01133+6434.....	136	95	77	4.62	51.5	121.7	100.4	26
02441+6922.....	236	164	62	15.23	21.2	15.0	17.1	26

adjusted the four *IRAS* band fluxes by the ratio of our observed flux to the *IRAS* flux at 25 μm (or at 12 μm if we only measured an upper limit at 25 μm). Five other sources are also normalized because the *IRAS* band 1-to-band 2 ratio is similar to the CFHT flux ratio although the sources are not clearly variable. Also plotted are the *JHKL* measurements by Whitelock and Feast (1984) of four of the 16 sources. No attempt has been made to adjust the *JHKL* measurements to take account of variability in the sources. Since all objects lie close to the plane of the Galaxy the possibility of confusion in the near-IR measurements cannot be entirely eliminated.

Examination of the infrared spectra of our 16 program sources shows that they can be divided into three classes: (i) those which show the 9.7 μm silicate feature in emission or absorption (class I); (ii) objects with an almost featureless blackbody-like continuum with color temperatures in the approximate range of 200–350 K (class II); (iii) objects which do not fit into either of the above two classes (class III).

Class I.—This class includes 19200+1536, 19288+2923, 19374+2359, 19386+1513, and 00170+6542. The first three show the 9.7 μm silicate feature in absorption and the last two show emission. Their dust color temperatures range from 250 to 350 K, which are similar to the color temperatures of known variable OH/IR stars (Olnon *et al.* 1984).

Class II.—This class can be further divided into subclasses (a) and (b). Class IIa are objects which spectrum peaks at $\lambda > 10$ μm, which includes 19454+2920 and 19477+2401. The other seven sources (00210+6221, 02441+6922, 19127+1717, 19548+3035, 19558+3333, 20103+3053, and 23268+6854) which are grouped into class IIb have higher color temperatures with their spectra peaking at wavelength shortward of 10 μm.

Class III.—The spectrum of 19520+2759 in Figure 3 shows that the energy distribution of this object is very broad and can be interpreted as a superposition of blackbodies of different temperatures. This suggests that the infrared emission originates from an extended cloud with a temperature gradient, similar to molecular clouds with embedded young stars (e.g., Lk Hα 101; Harvey, Thronson, and Gatley 1979). Another object, 01133+6434, has a very low color temperature of ~100 K (Fig. 3). The 25 μm *IRAS* measurement of this object is significantly higher than the corresponding CFHT measurement while the 12 μm point is not obviously discrepant. This suggests that the source may be larger than the CFHT beam at long wavelengths.

We performed a search of the *IRAS Low Resolution Spectra (LRS) Catalog* when it became available in 1985 and found eight of our 16 program sources to have *LRS* spectra. The *IRAS* low resolution spectrometer is a survey instrument operating in two overlapping wavelength ranges, one from 7.7 to 13.4 μm and the other from 11.0 to 22.6 μm at a resolution of $\lambda/\Delta\lambda \sim 40$. All sources in the *LRS* catalog are contained in the *Point Source Catalog* and the entire spectrum has been observed at least twice with consistent results. There is a total of ~5500 sources in the *LRS* catalog.

The *LRS* spectra for our eight sources are plotted in Figure 3 on the same scale as the other spectra. Good agreements are found between the *LRS* and CFHT measurements. In addition to the 9.7 μm silicate emission feature, the 18 μm emission feature is also clearly visible in 19386+1513 and 00170+6542. We also note the presence of an unidentified emission feature around 8 μm in 19520+2759, 23268+6854, and 00210+6221.

IV. DISCUSSION

What is the nature of these objects? It is clear that these sources in Circular No. 9 are quite diverse in character, and only five of the 16 are OH/IR stars as were originally suggested. We will discuss each of the 16 objects individually or in groups, with the results summarized in Table 4.

19200+1536, 19288+2923, 19374+2359, 10386+1513, and 00170+6542.—Four of the five objects in Class I are found to have double-peak OH emission (Engels *et al.* 1984; Lewis, Eder, and Terzian 1985) and three of the five have a variability probability of >80%. The almost exact correspondence between the infrared (silicate) and radio (OH) properties suggests that they are quite certain to be long-period oxygen-rich OH/IR stars. Both of the objects with the silicate feature in emission are visible on the Palomar Observatory Sky Survey (POSS) I print but two of the three with absorption features have no optical counterpart. This is consistent with the common belief that the self-absorbed silicate feature is the result of heavier circumstellar extinction.

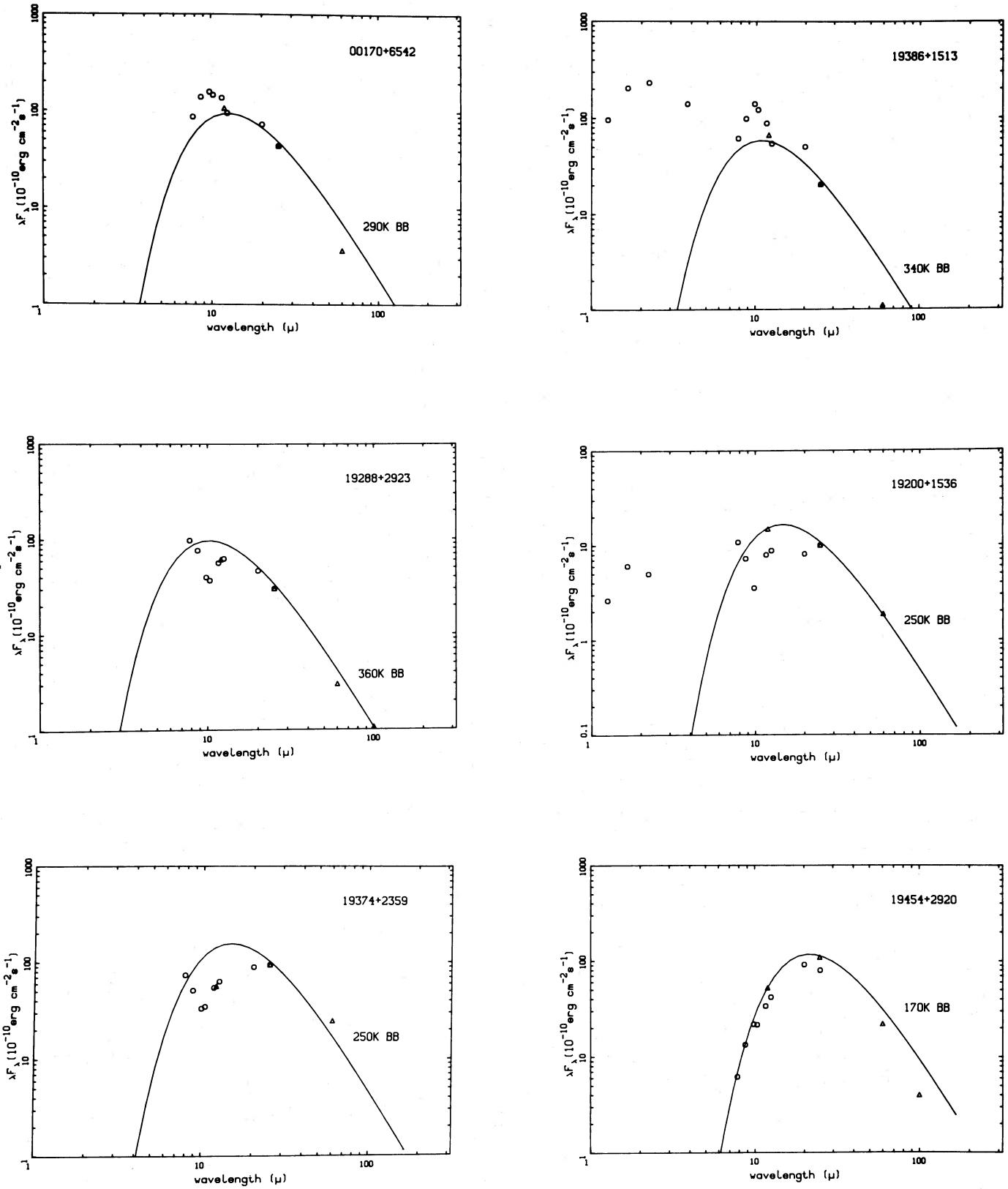

FIG. 1.—The infrared spectra of 00170+6542, 19386+1513, 19288+2923, 19200+1536, 19374+2359, and 19454+2920. The circles and triangles are CFHT and *IRAS* measurements, respectively. In 19386+1513 and 19200+1536 the near-infrared (*JHKL*) points of Whitelock and Feast (1984) are also plotted. Blackbody curves are shown in each spectra for comparison. In order to adjust for the effects of variability the *IRAS* points have been multiplied by a factor of 1.40, 0.66, 0.53, 0.83, and 0.78 for 00170+6542, 19386+1513, 19288+2923, 19200+1536, and 19374+2359, respectively.

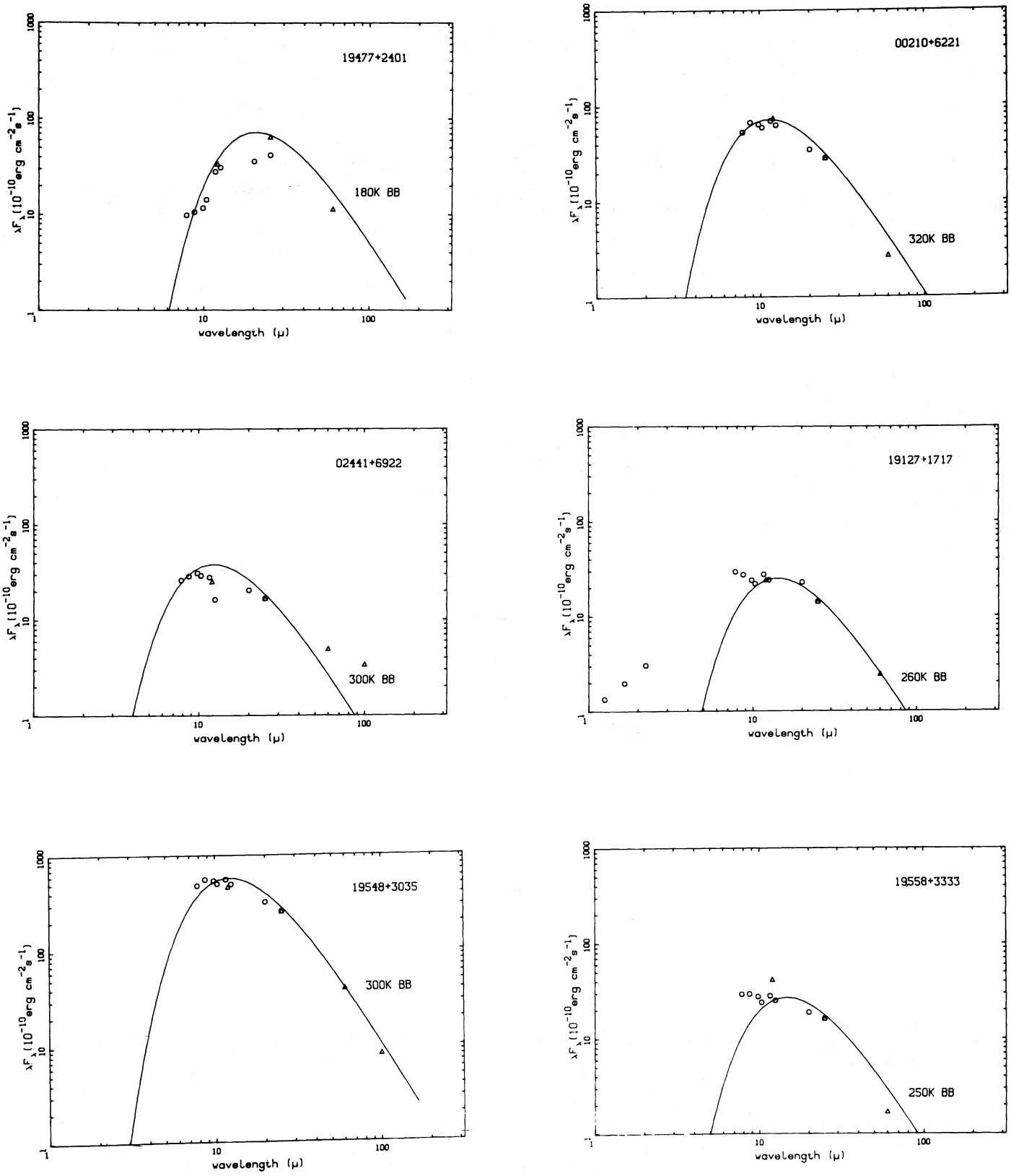

FIG. 2.—The infrared spectra of 19477+2401, 00210+6221, 02441+6922, 19127+1717, 19548+3035, and 19558+3333. The symbols are the same as in Fig. 1. The corresponding multiplying factors for 00210+6221, 02441+6922, 19127+1717, 19548+3035, and 19558+3333 are 0.56, 0.66, 0.68, 2.15, and 0.35. For 19127+1717 the near-infrared (*JHK*) points of Whitelock and Feast (1984) are also plotted.

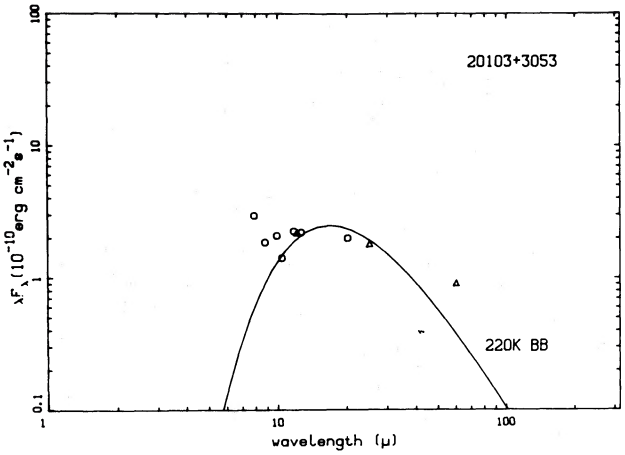

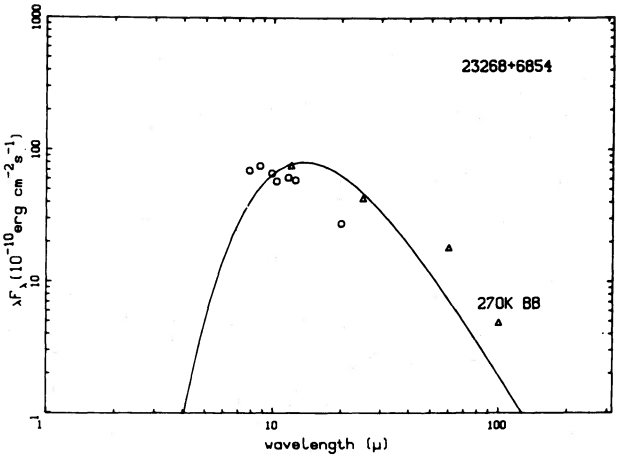

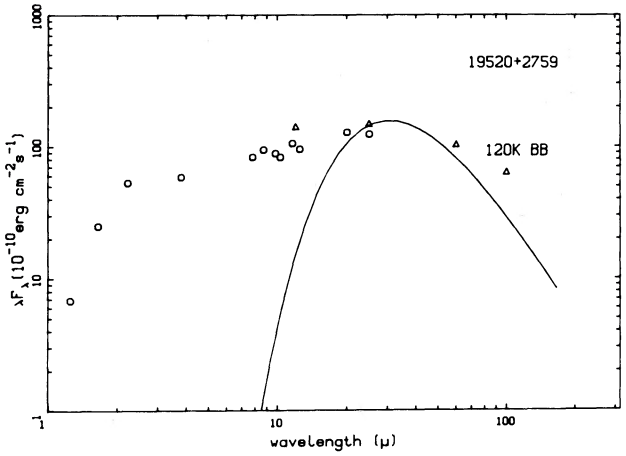

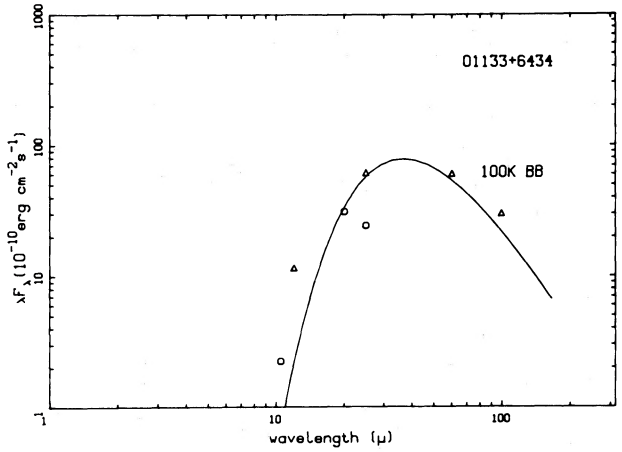

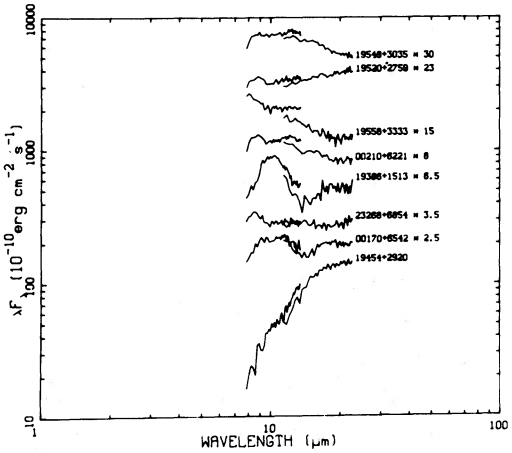

FIG. 3.—The infrared spectra of 20103 + 3053, 23268 + 6854, 19520 + 2759, and 01133 + 6434. For 19520 + 2759 the near-infrared (*JHKL*) points of Whitelock and Feast (1984) are also plotted. The *IRAS* points of 20103 + 3035 have been adjusted by a multiplying factor of 0.25. On a separate plot are the low-resolution spectra of eight of the Circular No. 9 sources.

TABLE 4

DERIVED PARAMETERS

Object	V_{LSR} (km s^{-1})	D (kpc)	Total Flux (ergs cm^{-2} s^{-1})	L_* ($L_\odot$)	M_c ($M_\odot$)	Suggested Classification
00170+6542.....	−51.5[a]	4	1.5 (−8)	7.8 (3)	0.65	OH/IR star
19386+1513.....	4.6[a]	0.5	4.1 (−8)	3.3 (2)	0.53	OH/IR star
19288+2923.....	−39.3[a]	12	9.6 (−9)	4.5 (4)	1.3	OH/IR star
19200+1536.....	59.5[a]	7	2.1 (−9)	3.4 (3)	0.58	OH/IR star
19374+2359.....			1.4 (−8)			OH/IR star
00210+6221.....	−38[b]	3	8.2 (−9)	2.4 (3)	0.56	PN?
19454+2920.....	13[b]	1, 7	1.0 (−8)	3.3 (2) − 1.6 (4)	0.53 − 0.79	Proto–PN
19477+2401.....	27[b]	3, 7	5.6 (−9)	1.6 (3) − 9.0 (3)	0.55 − 0.67	Proto–PN?
02441+6922.....	...	...	4.0 (−9)	...	...	?
19127+1717.....	...	...	4.2 (−9)	...	...	PN
19548+3035.....	...	...	7.1 (−8)	...	...	Carbon star
19558+3333.....	...	...	4.0 (−9)	...	...	Carbon star
20103+3053.....	...	...	4.2 (−10)	...	...	Carbon star
23268+6854.....	−34[b]	3	1.0 (1−8)	2.9 (3)	0.57	?
19520+2759.....	16.7[b]	9.5	3.4 (−8)	1.0 (5)	...	Young star
01133+6434.....	−52.8[b]	4	8.1 (−9)	4.2 (3)	...	Young star

[a] Engles *et al.* 1984.
[b] Arquilla, Leahy, and Kwok 1986.

A comparison with the color-color diagram of known OH/IR stars (Olnon *et al.* 1984) shows that the two sources with silicate emission lie in the area of visible Mira variables and the positions of two variable objects with silicate absorption features agree with the distribution of OH/IR stars. 19374+2359, a nonvariable object with the silicate feature in absorption, has a higher 60 μm to 25 μm flux ratio than the other four and has colors similar to known nonvariable OH/IR stars, which have been suggested to be OH/IR stars with detached dust shells (Bedijn 1986). The color temperature (~250 K) of 19374+2359 is certainly consistent with it being a more evolved object, and the fact that it has an optical counterpart suggests that the optical image may represent the emergence of the starlight from the diluted, detached dust shell as the star evolves to the blue side of the H-R diagram.

The nature of the Class II sources is less definite and possibly not homogeneous. Each object is discussed individually below.

00210+6221.—This object has a bright image in the POSS blue print. It has no obvious spectral feature in the 10 μm region and is classified by the *LRS* catalog as a star earlier than M5 (*LRS* class 12). Our CFHT measurements suggest that its spectrum peaks at ~10 μm and can be fitted by a blackbody of ~320 K. Broad CO line emission has been detected by Arquilla, Leahy, and Kwok (1986) and it probably has a carbon-rich envelope. While the nature of 00210+6221 cannot be definitely determined, its bright optical image suggests that it is more similar to a planetary nebula than an AGB star. If this is true, then its high dust temperature implies that it must be very young. The CO emission could originate from the remnant of its carbon-rich AGB progenitor. It would also be one of the very few planetary nebulae which are observed to have a molecular halo (Knapp 1985).

19454+2920 and 19477+2401.—These two objects have very similar dust temperatures ($T \sim 180$ K) and neither show definite variability. That they are heavily reddened by circumstellar extinction is evident by their extremely red color in the POSS prints. 19454+2920 has no optical counterpart at all and 19477+2401 is just visible on the I print. The *LRS* spectrum of 19454+2920 shows an almost perfect blackbody-like, featureless continuum. This contrasts with the common presence of strong infrared emission lines in planetary nebulae (e.g., NGC 7027). The absence of an optical image also suggests that a very small amount of ionized gas is present. The best-known proto–planetary nebula RAFGL 618 also has an almost featureless *LRS* spectrum with the exception of a broad unidentified dust feature around 8 μm. There is no sign of a photosphere under the dust continuum at $\lambda < 10$ μm in 19454+2920 and 19477+2401 as in the case for late-type stars. Both have been found (one tentatively) to have circumstellar CO emission (Arquilla, Leahy, and Kwok 1986) and are therefore likely to be very late carbon stars or in a stage of proto–planetary nebulae evolution (see § V).

02441+6922.—The spectrum of 02441+6922 shows an absorption feature around 12.5 μm, which could be due to a grain of unknown origin. We note also that the *IRAS* points are significantly higher than ours whereas the *IRAS* assigned probability of variability for this object is only 26%. We have no good suggestion regarding the possible nature of this object.

19217+1717.—Whitelock (1986) has found forbidden-line emission ([O III], [N II], [Ne II], [S III]) from 19127+1717 and suggests that it is a planetary nebula. It has previously been classified by Stephenson and Sanduleak (1977) as an emission-line object (SS 438). Like 00210+6221, 19127+1717 is very bright in the POSS blue print (Paper I) which is consistent with the above suggestion. The dust color temperature is, however, higher than most evolved planetary nebulae (Pottasch *et al.* 1984) but is not inconsistent with other candidates of young planetary nebulae (Kwok, Hrivnak, and Milone 1986). The probability of variability assigned by *IRAS* is 0% which is expected for a planetary nebula. The fact that the *IRAS* fluxes are higher suggest that the source may be larger than the 11″ beam of the CFHT.

19548+3035, 19558+3333, and 20103+3053.—The spectra of the rest of the class IIb objects are not as easily classified. These three sources have >90% probability of being variable and are therefore likely candidates of AGB stars. 19548+3035 (=RAFGL 2477) is another object in addition to 19127+1717, 19374+2359, and 00210+6221 which has an optical counterpart on the POSS O prints, and the published finding chart by Gosnell, Hudson, and Puetter (1979) agrees with ours in Paper I. Combining the near-infrared measurements of Gosnell,

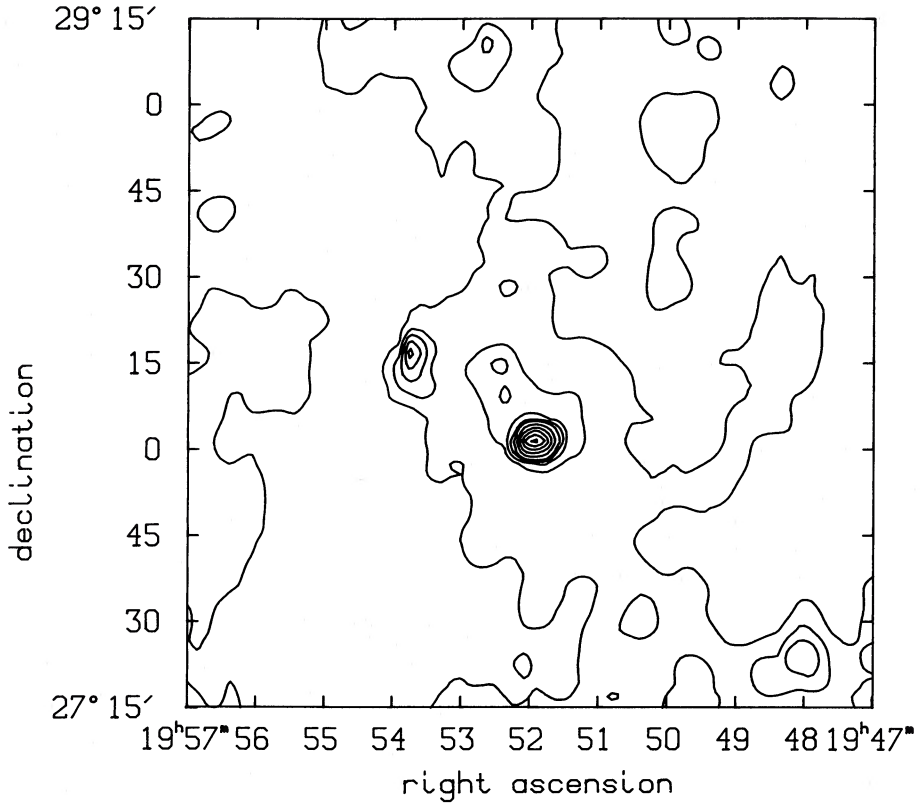

FIG. 4*a*

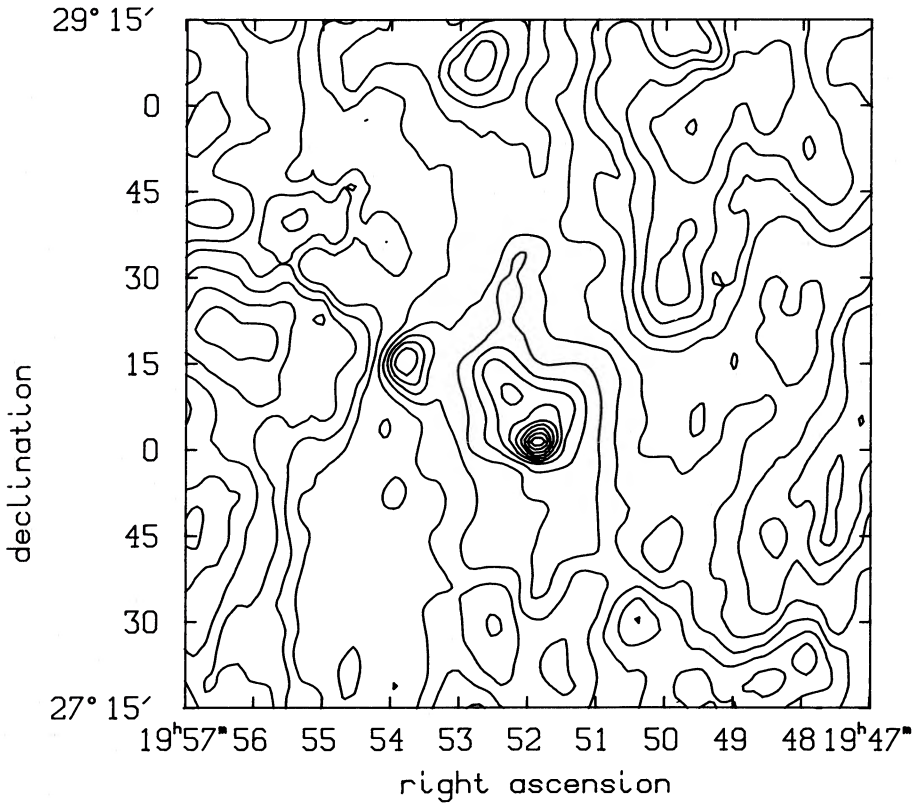

FIG. 4*b*

FIG. 4.—(*a*) *IRAS* 60 μm map of 19520+2759. (*b*) *IRAS* 100 μm map of 19520+2759. The contour intervals are at 5% of the peak value up to the 35% level and at 10% between 40% and 100%.

Hudson, and Puetter (1979) with those in this paper shows that the spectrum of 19548+3035 turns over at ~8 μm and its 300 K color temperature suggests that it may also be a reddened AGB star. In spite of its *LRS* classification of 21, no silicate feature is seen. 19558+3333 is classified by the *LRS* catalog as having a thick oxygen-rich envelope but there is no obvious 10 μm silicate feature present. We can only hypothesize that these three objects are carbon stars or they are oxygen-rich but their silicate feature is in transition from emission to absorption and therefore not detectable.

23268+6843.—The *LRS* spectral classification for 23268+6854 is that for a star earlier than M5. While this is supported by the short turnover wavelength (<8 μm), the 10–20 μm region is peculiarly flat. There is a significant discrepancy between the 20 μm CFHT flux and the 25 μm *IRAS* flux, again suggesting an extended source.

19520+2759.—Examination of the *IRAS* image files (Figs. 4*a* and *b*) shows that 19520+2759 is extended. CO observations by Arquilla, Leahy, and Kwok (1986) show extended CO emission around 19520+2759, and the infrared object is likely to be the energy source of the CO emission. Thus the object is likely to be a young star rather than a evolved star. Whitelock (1986) has detected Hα emission in this object, which is consistent with the suggestion that it is a young star with a compact H II region.

01133+6434.—This object is also found to be extended in both 60 and 100 μm bands (Figs. 4*a* and *b*). Arquilla, Leahy, and Kwok (1986) find extended CO emission over an area of >1.5 × 0.7 as well as evidence for a high-velocity outflow. This suggests that 01133+6434 is probably a site of recent star formation.

Table 4 summarizes the suggested classifications of the sources. At least two of the Circular No. 9 objects (01133+6434 and 19520+2759) are likely to be young stars rather than evolved stars. For those which have velocity information available from molecular line observations, kinematic distances are also estimated based on the galactic rotation model of Burton (1974). When these distances are combined with the observed total fluxes we are able to estimate the bolometric luminosities of the sources. The assumption that most of the stellar luminosity is emitted in the infrared is a good one for late-type stars, for the optical depth in the circumstellar envelope is often high. For evolved planetary nebulae, the low color temperature of the dust component is probably due to geometric dilution but not high optical depth and photons may be escaping in the form of far ultraviolet radiation.

For those sources which we believe to be AGB stars, proto–planetary nebulae, or planetary nebulae, we also derive the masses of the degenerate cores (M_c) based on the core mass luminosity relationship of Paczyński (1971). With the sole exception of 19288+2923 all core masses are consistent with those of intermediate mass stars. If the distance of 19288+2923 is correct then it may be a core-burning red supergiant rather than a shell-burning AGB star.

V. PROTOPLANETARY NEBULA EVOLUTION

In spite of the diverseness of the Circular No. 9 objects we believe that two objects in our observed sample (19454+2920 and 19477+2401) deserve particular attention for they may represent objects in a previously unobserved stage of stellar evolution.

The end of AGB evolution can be defined as the point where the envelope of the star begins to undergo rapid changes as the result of the depletion of the envelope mass due to mass loss. The value of this critical envelope mass ($M_\odot$) depends on the mass of the core (Paczyński 1971). For a star with a core mass of 0.6 $M_\odot$, Schönberner (1983) estimates M_e to be 10^{-3} $M_\odot$, corresponding to a stellar effective temperature of ~5000 K. It is also reasonable to assume that AGB mass loss stops at this point. During the subsequent evolutionary phase where the effective temperature of the star is between 5000 K and 30,000 K, the circumstellar envelope is not yet ionized and this period can be defined as the "proto–planetary nebulae" phase. Using the central star evolution model of Schönberner (1983), we can estimate that the lengths of the proto–planetary nebula phase are 1500, 1700, and 1500 yr for core masses of 0.64, 0.60, and 0.57 $M_\odot$, respectively. For lower core masses, this interval increases dramatically to values greater than the dynamical lifetime of planetary nebulae (Renzini 1983; Kwok 1985).

Since the remnant of the AGB circumstellar envelope continues to expand during the proto–planetary nebula phase, a proto–planetary nebula will be identified as a far-infrared object. The strength of the silicate feature (for those with oxygen-rich progenitors) will also decrease with time because of expansion (Kwok 1980). The color temperature of a proto–planetary nebula is expected to be lower than the temperature of the reddest AGB star but higher than that of a planetary nebula, i.e., in the range of 150–200 K.

Since all planetary nebulae go through the proto–planetary nebulae phase, we should expect the ratio of their respective lifetimes (1500 yr/[10,000 yr–30,000 yr]), or 5%–15%. The presence of >1000 planetary nebulae in the *IRAS Point Source Catalog* therefore implies that there are 50 to 150 heretofore unknown objects which are proto–planetaries. In order to identify these objects, we have adopted the following empirical criteria.

a) The *IRAS* interband color temperatures T_{12} and T_{23} should be in the range of 150–200 K.

b) The object should be nonvariable.

c) The silicate feature, if present, should be weak.

d) There should be no bright optical counterpart of the infrared source.

The above criteria are satisfied by both 19454+2920 and 19477+2401, although the latter has a weak image on the I plate. The detection of circumstellar CO emission from 19477+2401 leaves no doubt that it is a late-type object; if it is not a proto–planetary nebula then it must be in a very late stage of AGB evolution.

VI. CONCLUSIONS

We have obtained near infrared photometry for 16 of the *IRAS* Circular No. 9 objects. We are relatively certain that eight of the 16 are new evolved AGB stars—among which five are oxygen-rich OH/IR stars and the other three are probably carbon stars. The color temperatures of these stars range from 250–350 K. Such low color temperatures can be interpreted as the result of large optical depths of the circumstellar envelopes due to increasing mass loss. If this is the case then these stars could be the most evolved AGB stars ever studied.

Of the remaining eight objects, two are young stars in an early stage of formation. At least one, possibly two, are planetary nebulae. Most interestingly, there are two objects with very low color temperatures (~180 K) and no sign of being variable, and we suggest that they may correspond to a previously unobserved proto–planetary nebulae evolutionary phase.

We acknowledge with gratitude the help provided by Dr. R.

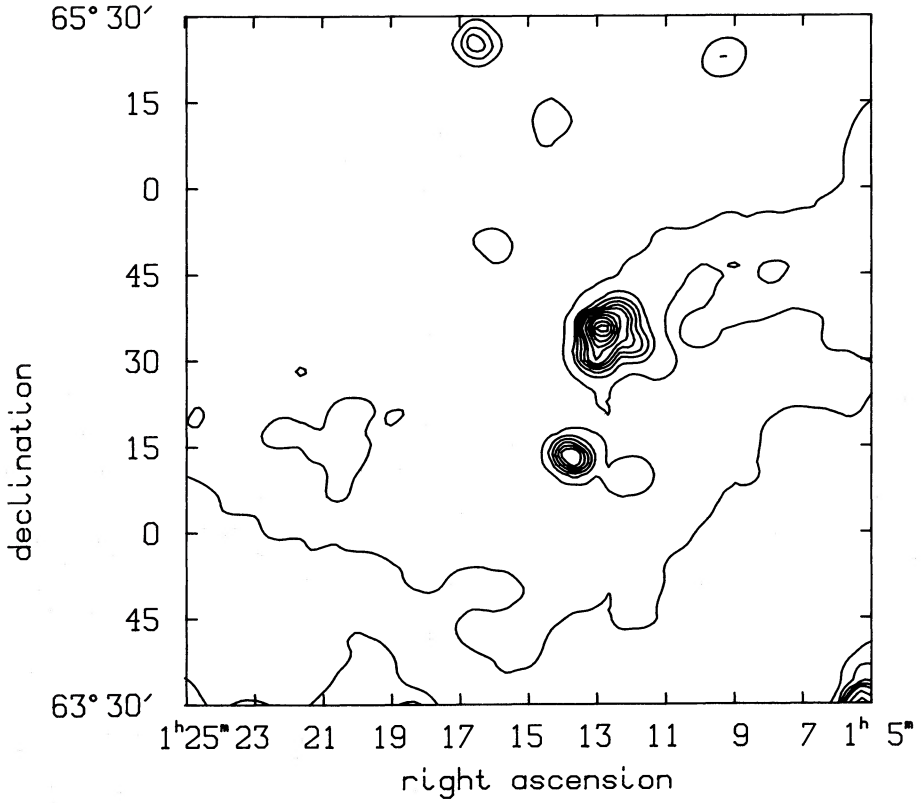

FIG. 5*a*

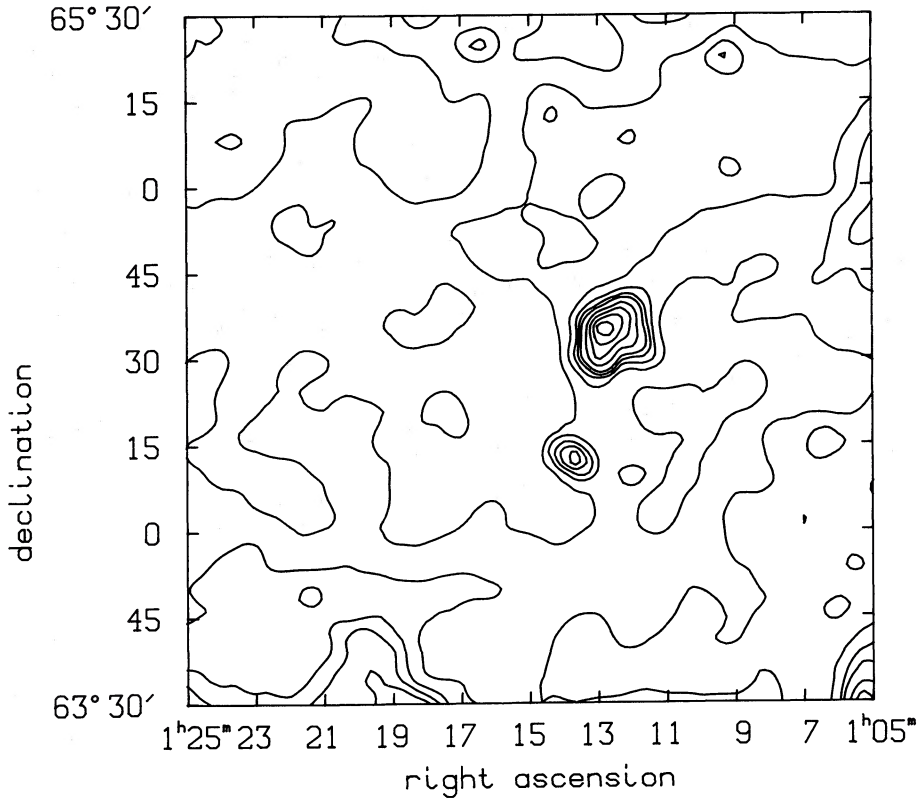

FIG. 5*b*

FIG. 5.—(*a*) *IRAS* 60 μm map of 01133 + 6434. (*b*) *IRAS* 100 μm map of 01133 + 6434. The contour levels are the same as Fig. 4.

A. McLaren at the CFHT. We thank the Dominion Radio Astrophysical Observatory for providing us with contour maps from the *IRAS* image files. University of Calgary undergraduates P. Langill and C. T. Haglund assisted in the data analysis. The *IRAS* catalogs are provided on magnetic tape in machine-readable form by the World Data Center in Greenbelt, Maryland. B. J. H. acknowledges the support of a grant from NASA administered by the American Astronomical Society. This work is in part supported by a grant to S. K. from the Natural Sciences and Engineering Research Council of Canada.

REFERENCES

Arquilla, R., Leahy, D. A., and Kwok, S. 1986, *M.N.R.A.S.*, **220**, 125.
Baud, B., Sargent, A. I., Werner, M. W., and Bentley, A. F. 1985, *Ap. J.*, **292**, 628.
Bedijn, P. J. 1986, in *Light on Dark Matters*, ed. F. P. Israel (Dordrecht: Reidel), p. 119.
Beichman, C. A., Neugebauer, G., Habing, H. J., Clegg, P. E., and Chester, T. J. 1985, *IRAS Catalogs and Atlases Explanatory Supplement* (Pasadena: Jet Propulsion Laboratory).
Burton, W. B. 1974, in *Galactic and Extra-Galactic Radio Astronomy*, ed. G. L. Verschuur and K. I. Kellerman (New York: Springer-Verlag), p. 82.
Engels, D., Kreysa, D., Schultz, G. V., and Sherwood, W. A. 1983, *Astra. Ap.*, **124**, 123.
Engels, D., Habing, H. J., Olnon, F. M., Schmid-Burgk, J., and Walmsley, C. M. 1984, *Astr. Ap.*, **140**, L9.
Gezari, D. Y., Schmitz, M., and Mead, J. M. 1984, *Catalog of Infrared Observations* (NASA Reference Publ. 1118).
Gosnell, T. R., Hudson, H., and Puetter, R. C. 1979, *A.J.*, **84**, 538.
Habing, H. J., and Olnon, F. M. 1984, *Nature*, **308**, 114.
Hanner, M. S., Tokunaga, A. T., Veeder, G. J., and A'Hearn, M. F. 1984, *A.J.*, **89**, 162.
Harvey, P. M., Thronson, H. A., Jr., and Gatley, I. 1979, *Ap. J.*, **231**, 115.
Herman, J., and Habing, H. J. 1985, *Astr. Ap. Suppl*, **59**, 523.
Hrivnak, B. J., Kwok, S., and Boreiko, R. T. 1985, *Ap. J.* (*Letters*), **294**, L113 (Paper I).
Knapp, G. R. 1985, in *Mass Loss from Red Giants*, ed. M. Morris and B. Zuckerman (Dordrecht: Reidel), p. 171.
Knapp, G. R., Phillips, T. G., Leighton, R. B., Lo, K-Y., Wannier, P. G., Wootten, H. A., and Huggins, P. J. 1982, *Ap. J.*, **252**, 616.
Kwok, S. 1980, *Ap. J.*, **236**, 592.
———. 1985, *Ap. J.*, **290**, 568.
Kwok, S., Hrivnak, B. J., and Milone, E. F. 1986, *Ap. J.*, **303**, 451.
Lewis, B. M., Eder, J., and Terzian, Y. 1985, *Nature*, **313**, 200.
Maillard, J. P., and Dyck, H. M. 1982, in *Proc. 2nd Infrared Workshop*, (Garching: ESO), p. 29.
Neugebauer, G., *et al.* 1984, *Ap. J.* (*Letters*), **278**, L1.
Olnon, F. M., Baud, B., Habing, H. J., de Jong, T., Harris, S., and Pottasch, S. R. 1984, *Ap. J.* (*Letters*), **278**, L41.
Paczyński, B. 1971, *Acta Astr.*, **21**, 4.
Pottasch, S. R., Baud, B., Beintema, D., Emerson, J., Habing, H. J., Harris, S., Houck, J., Tenningo, R., and Marsden, P. 1984, *Astr. Ap.*, **138**, 10.
Renzini, A. 1983, in *IAU Symp 103, Planetary Nebulae*, ed. R. D. Flower (Dordrecht: Reidel), p. 267.
Schönberner, D. 1983, *Ap. J.*, **272**, 708.
Stephenson, C. B., and Sanduleak, N. 1977, *Ap. J. Suppl.*, **33**, 459.
Tokunaga, A. J. 1984, *A.J.*, **89**, 1366.
Whitelock, P. A. 1986, in *Light on Dark Matter*, ed. F. P. Israel (Dordreicht: Reidel), p. 129.
Whitelock, P. A., and Feast, M. 1984, *M.N.R.A.S.*, **211**, 25P.

R. T. Boreiko: Space Science Laboratory, University of California, Berkeley, CA 94720

B. J. Hrivnak: Department of Physics, Valparaiso University, Valparaiso, IN 46383

Sun Kwok: Department of Physics, The University of Calgary, Calgary, Alberta, Canada T2N 1N4